

Yang, X., Chen, Q., Zeng, J., Zhang, J.S., and Shaw, C.Y. 2001. "A mass transfer model for simulating VOC sorption on building materials," *Atmospheric Environment*, 35(7), 1291-1299.

A MASS TRANSFER MODEL FOR SIMULATING VOC SORPTION ON BUILDING MATERIALS

X. YANG^{a*}, Q. CHEN^b, J.S. ZHANG^c, Y. AN^d, J. ZENG^d and C.Y. SHAW^d

^a Department of Civil, Architectural, and Environmental Engineering, University of Miami, Coral Gables, FL 33124-0630, USA

^b Building Technology Program, Massachusetts Institute of Technology, 77 Massachusetts Avenue, Cambridge, MA 02139, USA

^c Department of Mechanical, Aerospace & Manufacturing Engineering, Syracuse University, 147 Link Hall, Syracuse, NY 13244, USA

^d National Research Council of Canada, Institute for Research in Construction, Indoor Environment Program, M-24, Montreal Road, Ottawa, Ontario K1A 0R6, Canada.

Abstract - The sorption of VOCs by different building materials can significantly affect VOC concentrations in indoor environments. In this paper, a new model has been developed for simulating VOC sorption and desorption rates of homogeneous building materials with constant diffusion coefficients and material-air partition coefficients. The model analytically solves the VOC sorption rate at the material-air interface. It can be used as a "wall function" in combination with more complex gas-phase models that account for non-uniform mixing to predict sorption process. It can also be used in conjunction with broader indoor air quality studies to simulate VOC exposure in buildings.

Key word index: Numerical model, indoor air quality, diffusion coefficient, partition coefficient, environmental chamber, gypsum board.

Nomenclature

C_a	air phase VOC concentration [mg m^{-3}]
C_{ad}	adsorbed VOC concentration on the material surface [mg m^{-3}]
C_m	VOC concentration in the material film [mg m^{-3}]
D_a	VOC diffusion coefficient in the air [$\text{m}^2 \text{s}^{-1}$]
D_m	VOC diffusion coefficient in the material [$\text{m}^2 \text{s}^{-1}$]
g_i	component i of the gravitation vector [m s^{-2}]
K_l	Langmuir sorption coefficient [-]
K_{ma}	material-air partition coefficient [-]
L_m	thickness of the sorption material [m]
M	maximum number of roots for sorption
M_w	molecular weight of the compound [g mol^{-1}]
P	VOC vapor pressure [mmHg]
P_a	air pressure [Pa]
Pr	Prandtl number
q	VOC sorption rate [$\text{mg m}^{-2} \text{s}^{-1}$]
Q	VOC emission or sorption rate in the Laplace domain
s	Laplace operator
Sc	VOC Schmidt number
S_ϕ	source term for ϕ
T	absolute temperature [K]

* Corresponding author. Tel.: +305-284-3456; fax: +305-284-3492. E-mail address: xudongy@miami.edu

T_0	reference temperature [K]
u_j (j=1,2,3)	three components of air velocity
x_j (j=1,2,3)	coordinates
X_0	coefficient to calculate the sorption rate by a solid material
$X(j)$	system response under the unit triangle function $f(j\Delta\tau)$
y	direction of VOC sorption in the material

Greek Symbols

β	thermal expansion factor [K^{-1}]
τ	time [sec]
μ	molecular viscosity of air [Pa.s]
μ_i	roots of B(s) (see equation (17)), $\frac{\pi^2 i^2}{L_m^2} D_m$
ε_t	truncation error
$\Delta\tau$	time step [sec]
Γ_ϕ	effective diffusion coefficient for ϕ

Subscripts

a	air phase
j	spatial coordinate indices
m	sorption material

1. Introduction

Building materials have been acknowledged as a major emission source of volatile organic compounds (VOCs) indoors. Evidence from a variety of investigations and systematic studies suggests that building materials can also affect the transport and removal of indoor VOCs by sorption and desorption. Researchers have found that re-emission of sorbed VOCs can elevate VOC concentrations in the indoor environment (Tichenor et al., 1988; Bergland et al., 1988). Materials capable of depositing, adsorbing, and/or accumulating pollutants can influence indoor air quality during the entire service life of a building (Nielsen, 1987). Therefore, an accurate characterization of sorption of building materials and the sorption impact on indoor air quality is important.

At present, the studies of the sorption effect are mainly conducted by experiments using small-scale environmental chambers. In a typical chamber experiment, the material is placed in the chamber and exposed to a VOC source (a single VOC or VOC mixture) until a stable concentration of that VOC source in the test chamber is reached. The exposure is then stopped. The sorption of the material can be measured by monitoring the VOC concentration at the chamber outlet and comparing the results with the predicted concentration without the material.

Although the sorption of building materials can be detected by well-designed experiments, such studies are costly, time-consuming, and do not allow to scale-up the sorption data from one set of

environmental conditions (e.g., those in a small chamber) to others (e.g., those in a building). As a practical matter, it is obvious that we need to develop mathematical models to predict or estimate VOC sorption of building materials. To date, researchers have developed two types of sorption models: the equilibrium models and the kinetic models.

The equilibrium models assume that the sorption and desorption are confined on the material surface and an equilibrium is achieved between phases at the interface. The model parameters are obtained by fitting the model predictions with the experimental data using nonlinear regression method. Axley (1991) compared several equilibrium models that have been developed. Among those models, the most promising ones for examining the indoor environment are the Langmuir isotherm model and the linear isotherm model, a simplified asymptote of the Langmuir model at low VOC concentrations. The Langmuir isotherm model represents the equilibrium VOC concentrations on the material surface by:

$$C_{ad} = \frac{K_l C_a}{1 + K_l C_a} \quad (1)$$

At low gas phase concentration that is common in indoor environments, the Langmuir model can be simplified to a linear form as:

$$C_{ad} = K_l C_a \quad (2)$$

The isotherm models, together with the VOC mass balance in a test chamber, have been used to describe the sorption characteristics based on the chamber data (Dunn and Tichenor, 1988; Tichenor et al., 1991). These models, although simple in principle, have limitations. First, sorption on a building material involves several steps that transfer the VOCs from the bulk of the fluid phase to the specific sites within the interior of the material, as demonstrated in Figure 1. The mass transfer processes include interfacial mass transfer in the gas phase, sorption at the material-air interface, and for a permeable material, diffusion inside the material. Equilibrium models neglect both the interfacial mass transfer and the material-phase diffusion, whereas the latter could be an important mechanism governing the sorption of certain indoor materials (Little and Hodgson, 1996). The second limitation of the equilibrium models lies in their statistical nature: two or more model parameters must be obtained by fitting the model prediction with the experimental data using nonlinear regression routine. It has been found that given different initial estimations of model parameters, the fitted parameters may not be unique and the results may differ as much as a factor of 100 (De Bortoli et al., 1996; Zhang et al, 2000). Finally, most of the equilibrium models use the same set of experimental data to build the model and to evaluate the accuracy of the prediction; therefore, they have not been rigorously validated.

Kinetic models, on the other hand, take the VOC diffusion mechanisms into consideration. The parameters of kinetic models are the physical properties of materials. These parameters can be obtained independently from experiments rather than from curve fitting. Representative kinetic models are those developed by Axley (1991), Dunn and Chen (1993), and more rigorously, by Little and Hodgson (1996). Those models are, however, based on the largely untested assumption that indoor air is well-mixed. The use of such models are limited to simple cases

(e.g., a well-mixed room with single contaminant source and sink).

The objective of this paper is to develop a sorption model that can be used for more general, non-uniform mixing conditions. The model explicitly quantifies the essential mechanisms of VOC sorption, while maintaining the model itself in an analytically solvable form to provide a readily-accessible solution. The applicability of the sorption model is demonstrated by comparing the model prediction with experimental data from sorption experiments.

2. Model development

Consider the VOC mass transfer layers in air, material-air interface, and the material (Figure 2). To mathematically solve the sorption process, we make the following assumptions:

(1) Fick's law applies to mass diffusion in both air and the material.

(2) The material is homogeneous and the VOC diffusion coefficient in the material and the material-air partition coefficient are constant. Further, the VOC sorption occurs in a very thin layer of interior building materials. Hence the diffusion inside the material can be assumed to be 1-D.

(3) The mass transfer rate between the air and material is very small. Hence, the heat generation/release associated with the sorption is negligible.

With the above assumptions, the following section presents the governing equations of VOC mass transfer in these layers.

2.1. Governing equations in air, material-air interface, and the material

The VOC transport in the air is determined by diffusion through the boundary layer over the material-air interface. Hence, a complete set of airflow and VOC transport equations in the air phase are needed. For simplicity, the following discussion is confined to laminar flow (e.g., flow in a conventional small-scale chamber without a mixing fan). The general principle however applies to turbulent flow.

For an incompressible, laminar, and Newtonian flow, the conservation equations for continuity, momentum (using Boussinesq approximation for buoyancy), energy, and VOC species can be generalized as:

$$\frac{\partial}{\partial \tau}(\rho\phi) + \frac{\partial}{\partial x_j}(\rho u_j \phi) = \frac{\partial}{\partial x_j}(\Gamma_\phi \frac{\partial \phi}{\partial x_j}) + S_\phi \quad (3)$$

where

ϕ = 1 for mass continuity

ϕ = u_j ($j = 1, 2, \text{ and } 3$) for three components of momentum (u, v, w)

ϕ = T for temperature

$\phi = C_a$ for VOC concentrations

The ϕ , Γ_ϕ and S_ϕ are shown in Table 1.

At the material-air interface, VOC concentration changes from gas phase concentration in the air side, $C_a(0,\tau)$ (mg/m^3), to solid phase concentration in the material side, $C_m(0,\tau)$ (mg/m^3). At the equilibrium, the VOCs in the two phases are related through a sorption isotherm. In many simple cases, it can be assumed that the equilibrium follows the linear isotherm shown in equation (4):

$$C_m(0,\tau) = K_{ma}C_a(0,\tau) \quad (4)$$

where 0 means at the material-air interface ($y=0$). K_{ma} is the dimensionless material-air partition coefficient. Equation (4) is in consistent with the commonly used Langmuir isotherm model for low gas concentrations.

Most building materials are permeable to VOCs. VOCs adsorbed on such material surface will diffuse into the material. For a solid material with homogeneous diffusivity, the 1-D transient diffusion process is governed by:

$$\frac{\partial C_m(y,\tau)}{\partial \tau} = D_m \frac{\partial^2 C_m(y,\tau)}{\partial y^2} \quad (5)$$

where D_m is the VOC diffusion coefficient in the material (m^2/s), and y is the coordinate representing the direction that the VOC diffusion in the material occurs (m). The VOC mass transfer rate $q(y,\tau)$ ($\text{mg}/\text{m}^2\text{s}$) at an arbitrary displacement y of material and time τ is given by:

$$q(y,\tau) = -D_m \frac{\partial C_m(y,\tau)}{\partial y} \quad (6)$$

If the thickness of the material is L_m , the initial and boundary conditions for the solid material are:

$$C_m(y,\tau=0) = 0 \quad (7)$$

$$q(0,\tau) = -D_m \frac{\partial C_m(0,\tau)}{\partial y} = -D_a \frac{\partial C_a(0,\tau)}{\partial y} \quad (8)$$

$$C_m(L_m,\tau) = 0 \quad (9)$$

Equation (8) represents a mass balance at the material-air interface and equation (9) indicates two possibilities on the other side of the material ($y = L_m$). The first possibility is that the material is thick compared to the diffusion distance and the other side remains unaffected by the diffusion. The second is that the VOCs have already penetrated the material but the other side is not a perfect barrier to VOCs. In most cases, the diffusion process in a solid material is very slow and the first possibility exists. It should be mentioned that some researchers had assumed a non-permeable boundary condition at $y = L_m$. Such an assumption has been challenged by Fan and

Kokko (1995), who found that even when a diffusion tight facing (aluminum foil) was placed on the surfaces of an n-pentane-based foam sample, the aging process of the foam was still going on, indicating that the facing could not be perfectly diffusion tight. Apparently, further studies are desirable to determine the most appropriate boundary condition at $y = L_m$.

In general, the sorption process can be simulated by numerically solving the above governing equations. However, due to the extremely small magnitude of the diffusion coefficient of VOCs in materials, direct numerical simulation of VOC diffusion in materials requires very fine grids to determine the high VOC concentration gradients especially near the material-air interface. This can be avoided if the VOC sorption rate, $q(0,\tau)$, can be modeled based on the air phase concentration at the interface, $C_a(0,\tau)$, and the physical properties of the building material (see Figure 2). The model can then be used as a “wall function” in combination with more complex gas-phase model (e.g., equation (3)) to solve the sorption process. This forms the basic idea of the sorption model to be developed.

2.2. A new sorption model

By using the Laplace transformation, equations (5) and (6) can be rewritten as follows:

$$D_m \frac{\partial^2 C_m(y,s)}{\partial y^2} - s \cdot C_m(y,s) = 0 \quad (10)$$

$$Q(y,s) = -D_m \frac{\partial C_m(y,s)}{\partial y} \quad (11)$$

where s is the Laplace operator, $C_m(y,s)$ and $Q(y,s)$ are the Laplace transformation of $C_m(y, \tau)$ and $q(y, \tau)$, respectively.

The solution to equations (10) and (11) with the initial and boundary conditions (equations (4), (7), (8) and (9)) reads:

$$Q(0,s) = \frac{A(s)}{B(s)} C_a(0,s) \quad (12)$$

where $A(s) = K_{ma} \cosh\left(\sqrt{\frac{s}{D_m}} L_m\right)$ and $B(s) = \frac{1}{\sqrt{D_m s}} \sinh\left(\sqrt{\frac{s}{D_m}} L_m\right)$

Equation (12) is the response of the sorption rate to the air-phase concentration at the interface in the Laplace domain. The sorption rate in the time domain can be obtained by an inverse Laplace transformation of equation (12):

$$q(0, \tau) = L^{-1}\left[\frac{A(s)}{B(s)} C_a(0,s)\right] \quad (13)$$

Equation (13) is solvable if $C_a(0, \tau)$ is a simple function, e.g., a step or ramp function. However, in indoor environments, $C_a(0, \tau)$ is usually a complex function of time. A direct solution of equation (13) is generally not available. To solve the problem, we discretize the $C_a(0, \tau)$ into the sum of a series of discrete functions composed of the peak value at each sampling point multiplied by a unit triangle function, $f(j\Delta\tau)$ ($j = 0, 1, 2, \dots, n$), where $\Delta\tau$ is a time step. As shown in Figure 3, the sum of such a set of overlapping triangle functions is a first order approximation of $C_a(0, \tau)$. The sorption rate at a given time $n\Delta\tau$ is affected by the air-phase boundary concentration at time $n\Delta\tau$ as well as the boundary concentrations in the previous time, i.e.,

$$q(0, n\Delta\tau) = \sum_{j=0}^{n-1} X(j)C_a[0, (n-j)\Delta\tau] \quad (14)$$

where $X(j)$ is the system response under the unit triangle function $f(j\Delta\tau)$ ($j = 0, 1, 2, \dots, n$), and $C_a[0, (n-j)\Delta\tau]$ is the air phase boundary concentration at time $n\Delta\tau, (n-1)\Delta\tau, \dots, \Delta\tau$, respectively.

To calculate the system response at different time steps, we first obtain the system response under a unit ramp function:

$$g(\tau) = \frac{\tau}{\Delta\tau} \quad (15)$$

Based on equation (13), the system response under such a unit ramp function is:

$$G(\tau) = L^{-1}\left[\frac{A(s)}{B(s)} \frac{1}{s^2 \Delta\tau}\right] \quad (16)$$

$B(s)$ has an infinite number of real roots as follows:

$$s_i = -\mu_i = -\frac{\pi^2 i^2}{L_m^2} D_m, \quad i = 1, 2, 3, \dots \quad (17)$$

By using the Heaviside expansion (Beyer, 1975), equation (16) can be expressed as:

$$G(\tau) = \lim_{s \rightarrow 0} \frac{d}{ds} \left[s^2 \frac{A(s)}{B(s)} \frac{1}{s^2 \Delta\tau} e^{s\tau} \right] + \sum_{i=1}^{\infty} \frac{d}{ds} \left[\frac{A(s)}{[B(s) \cdot s^2] \Delta\tau} e^{s\tau} \right]_{s=-\mu_i} \quad (18)$$

From equations (17) and (18), we obtain:

$$G(\tau) = \frac{K_{ma} D_m \tau}{L_m \Delta\tau} + \frac{2K_{ma} L_m}{\pi^2 \Delta\tau} \sum_{i=1}^{\infty} \frac{1 - e^{-\mu_i \tau}}{i^2} \quad (19)$$

$X(0)$ is the response of $g(\tau)$ at time $\tau = \Delta\tau$:

$$X(0) = G(\Delta\tau) = \frac{K_{ma}D_m}{L_m} + \frac{2K_{ma}L_m}{\pi^2\Delta\tau} \sum_{i=1}^{\infty} \frac{1 - e^{-\mu_i\Delta\tau}}{i^2} \quad (20)$$

For calculating the response of $f(j\Delta\tau)$, $j=1, 2, \dots, n$, we decompose $f(j\Delta\tau)$ into the sum of three ramp functions as:

$$f(j\Delta\tau) = g[(j+1)\Delta\tau] - 2g[j\Delta\tau] + g[(j-1)\Delta\tau] \quad (21)$$

From equations (19) and (21), the system response at time $\tau = j\Delta\tau$ is then:

$$X(j) = G[(j+1)\Delta\tau] - 2G[j\Delta\tau] + G[(j-1)\Delta\tau] = \sum_{i=1}^{\infty} W_i e^{\mu_i\Delta\tau} e^{-\mu_i(j\Delta\tau)} \quad (22)$$

where $W_i = -\frac{2K_{ma}L_m}{\pi^2 i^2 \Delta\tau} (1 - e^{-\mu_i\Delta\tau})^2$.

Now we have the sorption rate at time $\tau = n\Delta\tau$:

$$q(0, n\Delta\tau) = X(0)C_a[0, n\Delta\tau] + \sum_{j=1}^{n-1} \left\{ \sum_{i=1}^{\infty} W_i e^{\mu_i\Delta\tau} e^{-\mu_i(j\Delta\tau)} C_a[0, (n-j)\Delta\tau] \right\} \quad (23)$$

Let $q_i(0, n\Delta\tau) = \sum_{j=1}^{n-1} W_i e^{-\mu_i(j\Delta\tau)} C_a[0, (n-j)\Delta\tau]$ be the sorption rate corresponding to the i^{th} root, we have:

$$q(0, n\Delta\tau) = X(0)C_a[0, n\Delta\tau] + \sum_{i=1}^{\infty} q_i(0, n\Delta\tau) \quad (24)$$

where $q_i(0, n\Delta\tau)$ is an unknown but can be obtained progressively as follows:

$$q_i(0, n\Delta\tau) = W_i C_a[0, (n-1)\Delta\tau] + e^{-\mu_i\Delta\tau} q_i[0, (n-1)\Delta\tau] \quad (25)$$

and initially, $q_i(0,0)=0$.

Equations (24) and (25) represent the new sorption model. Because the model links the material sorption rate to the VOC history in the air, it can take the VOC deposition on the material surface and the VOC diffusion in the material into account. Once the values of the D_m , K_{ma} , and the air phase concentration are determined, the sorption rate can be obtained by using the above model.

Since $B(s)$ has an infinite number of roots, there should be an infinite number of $q_i(0,\tau)$ terms corresponding to each root. However, equation (25) indicates that all the roots greater than some cut-off value have a negligible effect, because the contribution at a time step is always reduced

by a factor ($e^{-\mu_i \Delta \tau}$) of the previous sorption rate. If the truncation error is smaller than ε_t , namely,

$$e^{-\mu_i \Delta \tau} < \varepsilon_t \quad (26)$$

The maximum number of roots needed is:

$$M = \frac{L_m}{\pi} \sqrt{\frac{\ln(1/\varepsilon_t)}{D_m \Delta \tau}} \quad (27)$$

Equation (27) indicates that, the smaller the L_m and the bigger D_m , $\Delta \tau$, and ε , the fewer roots there will be. For example, if $L_m = 0.01$ m, $\varepsilon_t = 10^{-10}$, $\Delta \tau = 60$ s, and $D_m = 2.5 \times 10^{-12}$ m²/s, which is common for a solid material, the total number of roots will be less than 1250.

3. Model evaluation

To evaluate a model objectively, the data used for the evaluation process should be independent of the data used to develop the model. Common practice of curve-fitting, which are largely used to develop the equilibrium models, should be avoided. In the following, the new sorption model is incorporated into a numerical code to simulate the dynamic sorption process. The simulation will reproduce the results of the sorption experiments. The simulated results are then compared with the experimental data for validation.

3.1. Sorption data from a small-scale test chamber

To validate the sorption model, we first measured the VOC sorption on an unpainted gypsum board using an environmental test chamber. The 0.05 m³ environmental chamber, shown in Figure 4, is made by stainless steel. Three VOCs, which represent alkanes, ketones, and chlorine-substituted compounds, were tested for their sorption and desorption characteristics. They are ethylbenzene, benzaldehyde, and dodecane. Table 2 gives the molecular weight and some physicochemical properties of the compounds used to determine the diffusion and partition coefficients.

For each test, a specimen holder was used to confine the sorption to the top surface; the surface area was 0.2×0.45 m². The edges of the materials were sealed with wax. After waxing the edges, the specimen in the holder was kept in a well-ventilated cabinet for over two weeks. As the emission of the wax diminished, the specimen in the holder was placed in the test chamber and conditioned with clean air. Test started after the background VOC concentration of the chamber air fell below 1 $\mu\text{g}/\text{m}^3$.

At the start of each test, the testing VOC was injected into the inlet flow. The material was placed in the chamber and exposed to the VOC source. The sink strength of the material was indicated by the difference of VOC concentrations between the inlet and outlet (we refer to this stage as the sorption phase). Once an apparent stable concentration of that VOC in the test chamber was reached, the exposure was stopped. Again, by monitoring the VOC concentration

for a period of time, the desorption of the VOC by the material was measured. During the experiments, the chamber air samples were collected by adsorption tubes and analyzed by a gas chromatography with a flame ionization detector (GC/FID). The test conditions were:

- Temperature: 23 ± 1 °C
- Relative humidity: 50 ± 2 %
- Air exchange rate: 0.5 ± 0.01 h⁻¹
- Chamber loading factor: 0.57 m²/m³

The material properties that are required by the sorption model were obtained from the literature. Bodalal *et al.* (1999) experimentally measured the diffusion coefficient and partition coefficient of the unpainted gypsum board and gave the following correlations for D_m (m²/s) and K_{ma} :

$$D_m = \frac{3.32 \times 10^6}{3600 M_w^{6.6}} \quad (28)$$

$$K_{ma} = 10600 / P^{0.91} \quad (29)$$

From equations (28) and (29), the D_m and K_{ma} for each compound can be calculated, as shown in Table 3. After obtaining these parameters, we can simulate the sorption and compare the predicted results with the measured data.

3.2. Simulation of VOC sorption on unpainted gypsum board and comparison with the data

To simulate the sorption process, the sorption model (equations (24) and (25)) was incorporated into a numerical code to simulate the air phase concentration with the presence of the material (gypsum board). Since VOC sorption has a negligible impact on airflow, the numerical simulation of the above process was conducted in two separate steps. First, a commercial CFD (computational fluid dynamics) program (CHAM, 1996) was used to simulate the airflow and obtain the steady-state distributions of air velocity. The flow results were then incorporated into the VOC mass-transfer equations (equation 3 with $\phi=C_a$) for simulating the dynamic sorption process. This procedure involved the coupling between air region, the interface, and the material (sorption model). Details of the procedure are given by Yang (1999).

The numerical simulation revealed time-dependent, spatial VOC distributions in the chamber. Since the measurement (sampling) point was at the chamber outlet, the following discussion is focused on the results at that particular location.

Figure 5 shows the comparison of the VOC concentrations at the chamber outlet for the model predictions and the chamber observations for ethylbenzene, benzaldehyde, and dodecane, respectively. In general, the predicted concentrations during the sorption phase (0 - 310 hours) and desorption phase (310 - 500 hours) agree with the measured data. However, different compounds have different discrepancies. For both ethylbenzene and benzaldehyde, the model tends to over-predict the strength of both sorption and desorption, resulting in lower chamber concentrations during the sorption phase and higher concentrations during the desorption phase.

The dodecane behaves just the opposite, and the model tends to underestimate the strength of sorption.

The discrepancies between the predicted and measured concentrations may be due to two different reasons. First, An et al. (1999) found that the chamber walls themselves also had a considerable sink effect, especially for compounds with low vapor pressure. This may partly explain the discrepancy between the predicted and measured results for dodecane, but not for ethylbenzene and benzaldehyde. The discrepancies for the latter compounds may be primarily due to the possible inaccurate values used for the D_m and K_{ma} , which actually determine the sorption. For example, a much better agreement for benzaldehyde can be achieved by using $D_m = 2 \times 10^{-12} \text{ m}^2/\text{s}$ and $K_{ma} = 3000$, as illustrated in Figure 6. It is clear that an accurate method to obtain D_m and K_{ma} is essential for the further validation of the sorption model.

To evaluate the strength of the material on sorbing or desorbing VOCs, Figure 7 gives the percentage of the total incoming VOC rate (from the inlet air) uptaken during the sorption period. The figure also gives the amount of VOCs released (represented by the percentage of the VOC rate released to the total VOC rate from the inlet during the sorption phase) during the desorption period. The results indicate that the gypsum board can uptake a significant portion of the VOCs. At the beginning, about 25% (for ethylbenzene) to 55% (for dodecane) of the VOCs from the inlet air was sorbed by the material. At 310 hours, the percentage dropped to 3.9% for ethylbenzene and 11.5% for dodecane. From 310 hours, the supply VOCs stopped and the material began to release the adsorbed VOC to the air and serve as a secondary source. At the beginning of the desorption phase ($\tau=315$ hours), the release rate was about 20% (of the VOC rate from the inlet during the sorption phase) for ethylbenzene and 32% for dodecane. As time passed, the release rate decreased but this would last a long period of time.

4. Conclusions

A model has been developed for VOC sorption on homogeneous building materials with a constant diffusion coefficient and partition coefficient. The model solves analytically the VOC sorption rate at the material-air interface as a function of the air-phase concentration. The model carries information on the physical representation of the entire sorption process. The sorption model has been incorporated into a numerical program to study VOC sorption on an unpainted gypsum board. Results show that the model can simulate the general trend of the sorption curve.

The new sorption model can be used as a “wall function” in combination with more complex gas-phase models that account for non-uniform mixing to predict sorption process. It can also be used in conjunction with broader indoor air quality studies to simulate VOC exposure in buildings. To successfully use the sorption model developed, research focused on the accurate measurement of the diffusion coefficient and partition coefficient is highly needed.

Acknowledgements

This investigation is supported by the US National Science Foundation (Grant CMS-9623864) and National Research Council of Canada. The authors also thank two anonymous reviewers for their insightful comments.

References

- An, Y., Zhang, J.S., Shaw, C. Y., 1999. Measurements of VOC adsorption /desorption characteristics of typical interior building material surfaces. *International Journal of HVAC&R Research* (in Press).
- Axley, J.W., 1991. Adsorption modeling for building contaminant dispersal analysis. *Indoor Air* 1, 147-171.
- Berglund, B., Johansson, I., Lindvall, T., 1988. Adsorption and desorption of organic compounds in indoor materials. In *Proceedings of Healthy Buildings'88* 3, 299-309.
- Beyer, W.H., 1975. *Handbook of Mathematical Sciences*, 5th Edition. CRC Press, Inc.
- Bodalal, A., Zhang, J.S., Plett, E.G., 1999. Method for measuring internal diffusion and equilibrium partition coefficients of volatile organic compounds for building materials. *Building and Environment* 35 (2), 101-110.
- De Bortoli, M., Knoppel, H., Colombo, A., Kefalopoulos, S., 1996. Attempting to characterize the sink effect in a small stainless steel test chamber. *Characterizing sources of indoor air pollution and related sink effects* ASTM STP 1287, American Society of Testing and Materials, Philadelphia, 307-320.
- Dunn, J., Tichenor, B.A., 1988. Compensating for sink effects in emissions test chambers by mathematical modeling. *Atmospheric Environment* 22, 885-894.
- Dunn, J.E., Chen, T., 1993. Critical evaluation of the diffusion hypothesis in the theory of porous media VOC sources and sinks. *Modeling indoor air quality and exposure*, ASTM STP 1205, American Society of Testing and Materials, Philadelphia, 64-80.
- Fan, Y., Kokko, E., 1995. Potential improvement of n-pentane-based foam insulation. *Journal of Cellular Plastics* 31, 217-226.
- Little, J.C., Hodgson, A.T., 1996. A strategy for characterizing homogeneous, diffusion-controlled, indoor sources and sinks. *Characterizing sources of indoor air pollution and related sink effects*, ASTM STP 1287, American Society of Testing and Materials, Philadelphia, 294-304.
- Nielsen, P., 1987. Potential pollutants – their importance to the Sick Building Syndrome –and their release mechanism. In *Proceedings of Indoor Air'87* 2, 598-602.
- Tichenor, B.A., Sparks, L.E., White, J., Jackson, M., 1988. Evaluating sources of indoor air pollution. Paper presented at 81st Annual Meeting of the Air Pollution Control Association, Dallas, TX.
- Tichenor, B.A., Guo, Z., Dunn, J.E., Sparks, L.E., Mason, M.A., 1991. The interaction of vapor phase organic compounds with indoor sinks. *Indoor Air* 1, 23-35.
- Yang, X., 1999. *Study of building material emissions and indoor air quality*, Ph.D. Thesis, Massachusetts Institute of Technology, Cambridge, Massachusetts.
- Zhang, J, Zhang, J.S., Chen, Q., Yang, X., 2000. A critical review on sorption models. In *Proceedings of Health Building'2000* (in Press).

Table 1 Values of ϕ , Γ_ϕ and S_ϕ in equation (3).

ϕ	Γ_ϕ	S_ϕ
1	0	0
u_i (i=1,2,3)	μ	$-\frac{\partial P_a}{\partial x_i} - \rho g_i \beta(T - T_0)$
T	μ/Pr	S_T
C_a	μ/Sc	S_c

Table 2 Selected compounds and their physicochemical properties.

VOCs	Molecular weight	Boiling point (°C)	Vapor pressure (mmHg)
Ethylbenzene	116.25	136.3	8.27
Benzaldehyde	253.21	178	1.06
Dodecane	170.34	216	0.27

Table 3 D_m and K_{ma} for simulating VOC sorption on unpainted gypsum board.

Compound	Ethylbenzene	Benzaldehyde	Dodecane
D_m (m ² /s)	2.154×10^{-11}	3.932×10^{-11}	1.73×10^{-12}
K_{ma}	1550	10053	34895

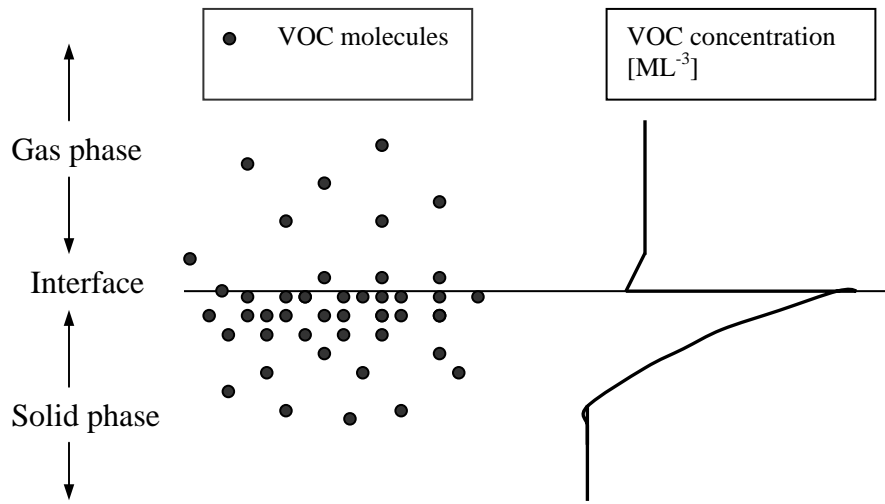


Figure 1 Schematic of the general mass transfer regions of an adsorption process.

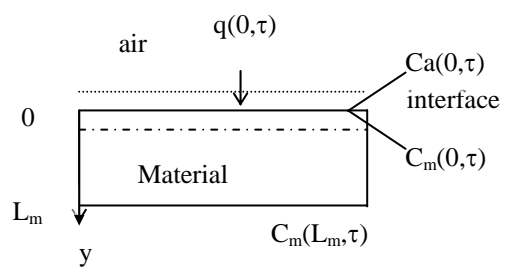


Figure 2: VOC sorption on a solid material

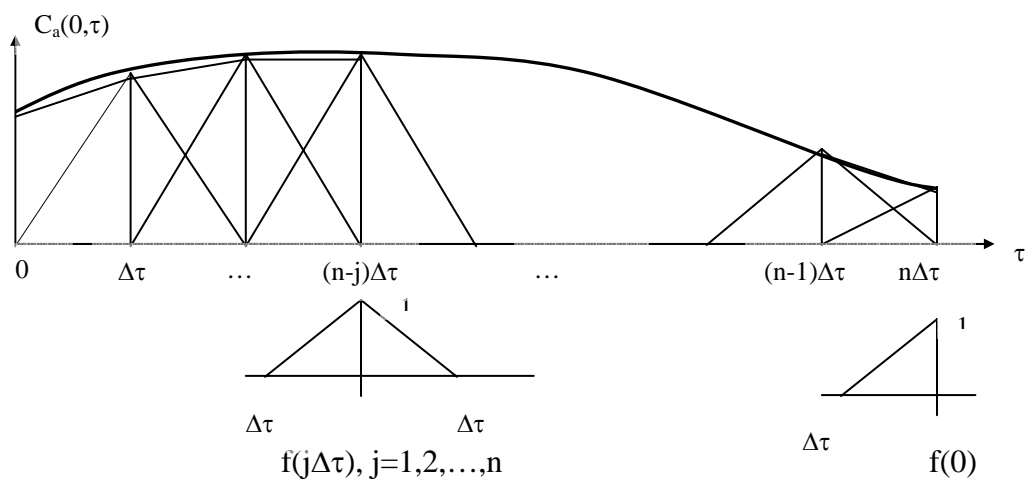


Figure 3 Discretization of the $C_a(0,\tau)$ with a series of unit triangle functions.

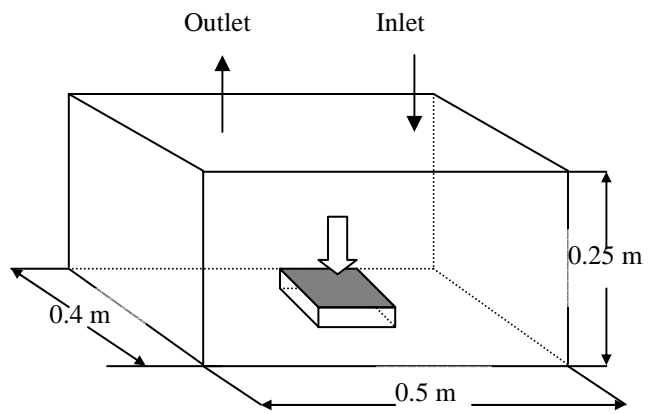
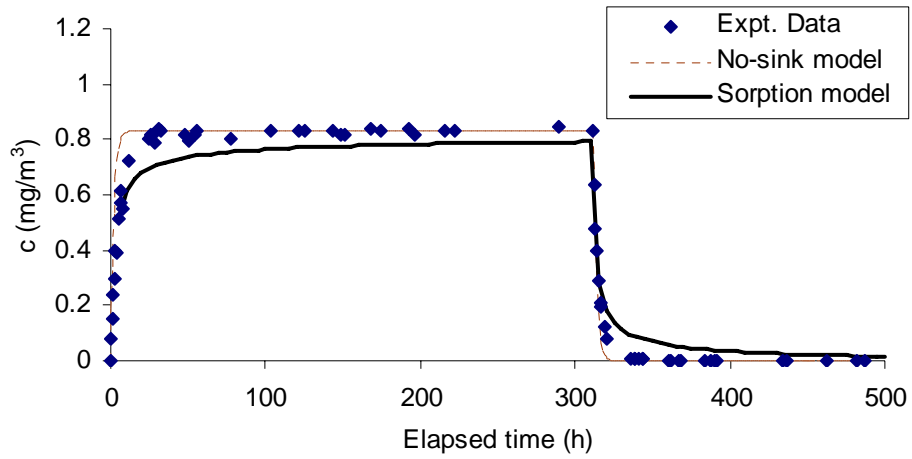
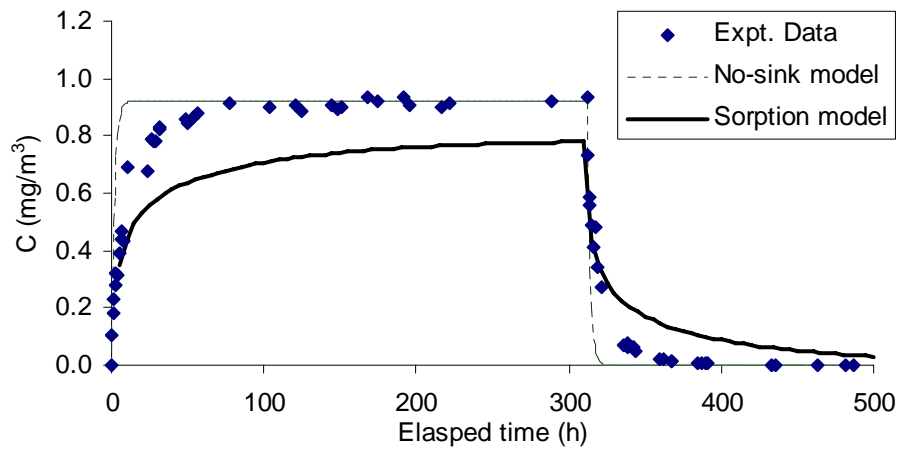


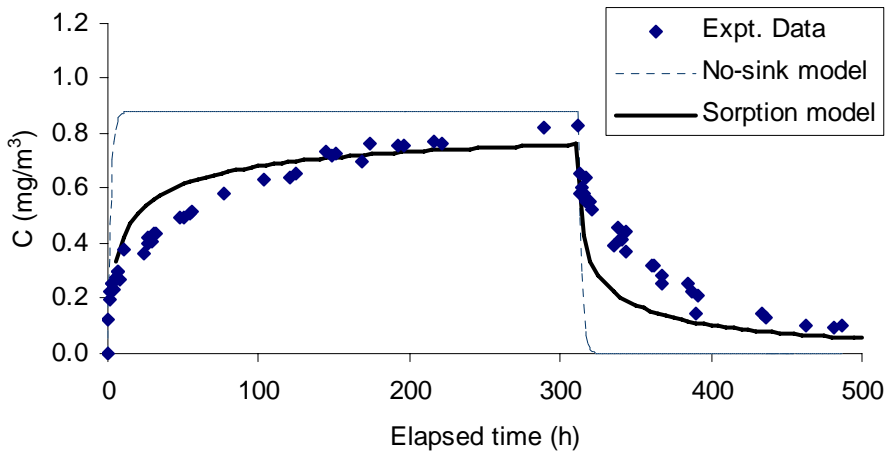
Figure 4 A small-scale chamber for measuring VOC sorption on a solid material.



(a)



(b)



(c)

Figure 5 Comparison of measured and simulated sink effects of unpainted gypsum board: (a) Ethylbenzene, (b) Benzaldehyde, (c) Dodecane.

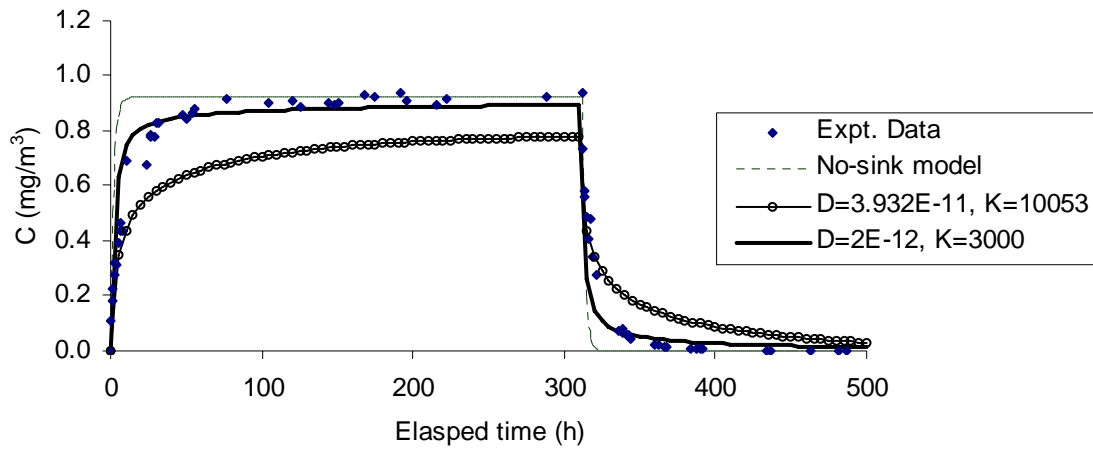


Figure 6 A better agreement between the model prediction and experiment can be achieved by adjusting the material properties (D_m and K_{ma}). The results shown here are benzaldehyde sorption on unpainted gypsum board.

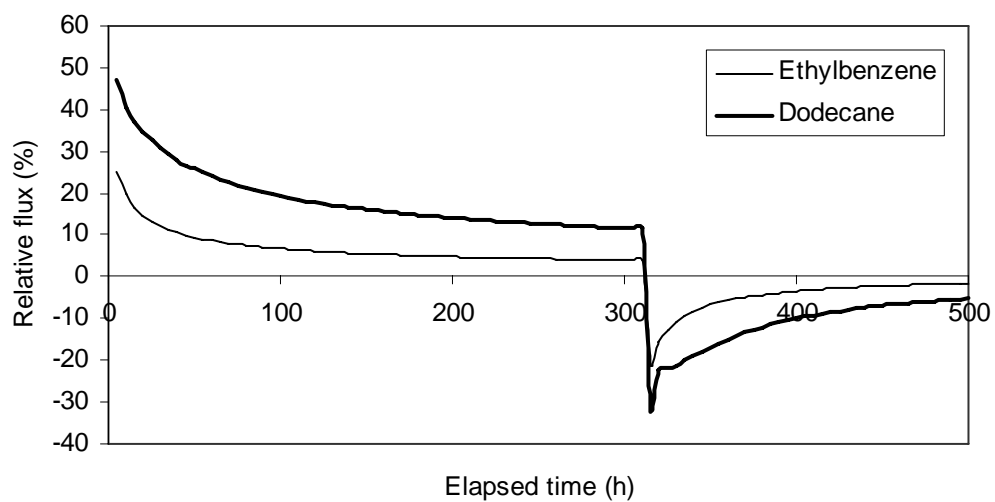


Figure 7 Simulated sink effect for ethylbenzene and dodecane by unpainted gypsum. Results show the percentage of the incoming VOC rate (from the inlet air) uptaken during the sorption period (0-310 h) and the VOCs released (represented by the percentage of the VOC rate released to the total VOC rate from the inlet during the sorption phase) during the desorption period (> 310 h).

Figure caption:

Fig. 1. Schematic of the general mass transfer regions of a sorption process.

Fig. 2. VOC sorption on a solid material

Fig. 3. Discretization of the $C_a(0,\tau)$ with a series of unit triangle functions.

Fig. 4. A small-scale chamber for measuring VOC sorption on a solid material.

Fig. 5. Comparison of measured and simulated sink effects of unpainted gypsum board: (a) Ethylbenzene, (b) Benzaldehyde, (c) Dodecane.

Fig. 6. A better agreement between the model prediction and experiment can be achieved by adjusting the material properties (D_m and K_{ma}). The results shown here are benzaldehyde sorption on unpainted gypsum board.

Fig. 7. Simulated sink effect for ethylbenzene and dodecane by unpainted gypsum. Results show the percentage of the incoming VOC rate (from the inlet air) uptaken during the sorption period (0-310 h) and the VOCs released (represented by the percentage of the VOC rate released to the total VOC rate from the inlet during the sorption phase) during the desorption period (> 310 h).